ResearchGate

See discussions, stats, and author profiles for this publication at: https://www.researchgate.net/publication/229860403

Electronic Structure of the BF 2 Radical Determined by ab Initio Calculations and Resonance-Enhanced Multiphoton Ionization Spectroscopy

ARTICLE *in* THE JOURNAL OF PHYSICAL CHEMISTRY A · MARCH 1997

Impact Factor: 2.69 · DOI: 10.1021/jp9623251

CITATIONS
8

READS
10

3 AUTHORS, INCLUDING:

Jeffrey W Hudgens
National Institute of Standards and Technolo…
135 PUBLICATIONS **2,251** CITATIONS

SEE PROFILE

Available from: Jeffrey W Hudgens
Retrieved on: 23 January 2016

Electronic Structure of the BF_2 Radical Determined by *ab Initio* Calculations and Resonance-Enhanced Multiphoton Ionization Spectroscopy

Dean B. Atkinson,[†] Karl K. Irikura,*[,‡] and Jeffrey W. Hudgens*[,§]

Physical and Chemical Properties Division, National Institute of Standards and Technology, Gaithersburg, Maryland 20899

Received: July 31, 1996; In Final Form: November 15, 1996[⊗]

We report the first electronic absorption spectrum of the boron difluoride radical. This spectrum appeared in mass-selected multiphoton ionization spectra between 235 and 420 nm. Strong bent−linear structure changes prevented observations of electronic origin bands. EOM-CCSD *ab initio* calculations suggest that the observed vibrational bands arise from $\tilde{A}\,^2B_1 \leftarrow \tilde{X}\,^2A_1$ (T_{vert} = 35 100 cm^{-1}) one-photon absorption and from $\tilde{B}\,^2A_1$ (3s) ←← $\tilde{X}\,^2A_1$ (T_{vert} = 59 100 cm^{-1}) and $\tilde{C}$ (3p) ←← $\tilde{X}\,^2A_1$ (T_{vert} = 63 100 cm^{-1}) two-photon transitions. *Ab initio* calculations predicted the geometries and vibrational frequencies of the ground states of the BF_2 radical, cation, and anion. *Ab initio* calculations also predicted the vertical transition energies to the excited electronic states from the ground state radical. QCISD(T) calculations estimate ionization potentials for BF_2 radicals of IP_a = 8.66 eV and IP_v = 10.44 eV and adiabatic and vertical electron detachment energies for BF_2^- of EA = 1.14 eV and VDE = 1.64 eV. We estimate these ionization and detachment energies to be reliable to about 0.05 and 0.10 eV, respectively.

Introduction

We report the first electronic absorption spectra of BF_2 radicals. These spectra were observed using resonance-enhanced multiphoton ionization (REMPI) spectroscopy. To support the analyses of these spectra, we also report high-level *ab initio* calculations for BF_2, BF_2^+, and BF_2^-. The REMPI spectra presented here form the basis of a very sensitive optical detection method for gas-phase BF_2 radicals. These results have practical application for studies of chemical reactions involving BF_2, many of which have commercial importance to the semiconductor industry. Simple compounds of boron, including BF_2 species, are used in a variety of applications relating to chemical vapor deposition (CVD). BF_2 also appears during the bulk deposition of boron nitride as a hardener on semiconductor surfaces.[1−3] More recently, BF_2^+ ion implantation has been used to form very thin p^+/n semiconductor junctions.[4−7]

Limited spectroscopic data are available for BF_2. Infrared spectra of BF_2 radicals and cations entrained in cryogenic matrices have established most of the fundamental vibrational frequencies.[8,9] The ESR spectrum reported by Nelson and Gordy indicates that $BF_2(\tilde{X}\,^2A_1)$ has a bent structure with ∠F−B−F = 112°;[10] however, most electronically excited states of BF_2 are linear. The bent−linear geometry change that accompanies electronic excitation frustrates spectroscopic studies by making the vibrational structure complex and the origin band intensity vanishingly weak. To date, electronic spectra attributed to BF_2 have been obtained by high-energy excitation of BF_3 molecules followed by observation of the dispersed fluorescence.[11−14] Creasey et al.[11] recorded an emission spectrum of BF_2 between 220 and 290 nm. They attributed the spectrum to emissions from the $1\,^2B_1$ state and suggested that the spectrum may include contributions from the $2\,^2A_1$ state. The energy of the emitting states was not determined.

Most information on the structure and excited states of the BF_2 molecule has come from *ab initio* theoretical calculations.[15−22] In this work we use the results of *ab initio* calculations to deduce spectroscopic assignments of REMPI spectra. We present high-level *ab initio* calculations which predict the geometries, vibrational frequencies, and energetics of ground state BF_2, BF_2^+, and BF_2^- and also the vertical excitation energies from the ground state of BF_2 to its lower energy valence and Rydberg states. To aid the spectroscopic assignments, we also make use of the multireference singles and doubles configuration interaction (MRD-CI) calculations by Perić and Peyerimhoff, who have predicted the vibrational frequencies of the lower valence and Rydberg states.[15,16] The MRD-CI calculations explicitly accounted for some of the many perturbations among the different vibrational levels of the electronic states.

Computational Procedures and Results

The ground-state geometries and harmonic vibrational frequencies of BF_2, BF_2^+, and BF_2^- were determined using the 6-311+G* basis set (66 contracted basis functions, cGTOs) at the frozen-core QCISD(T)[23,24] and hybrid density-functional B3LYP[25] levels of theory. Vertical excitation energies in the neutral radical, at the B3LYP geometry, were computed in the frozen-core approximation at the well-correlated EE-EOM-CCSD level of theory[26] and also at the uncorrelated, singles-only configuration interaction (CIS) level. Rydberg states have a simple electronic structure and are well described using such single-reference theories, but valence states may be more complicated. Thus the vertical excitation energies to valence states were also calculated at the multireference CASPT2-(13,13) level[27] (involving more than 300 000 configuration state functions in the CASSCF reference). The weight of the CASSCF reference was about 0.92 in each CASPT2 wave function obtained. Valence-state excitation energies were also calculated using the B3LYP method; density functional procedures are often surprisingly effective in systems with substantial nondynamical correlation. The aug-cc-pVTZ basis sets,[28,29] supplemented by a set of diffuse d-functions (α = 0.016) on boron, which we denote as aug-cc-pVTZ+d(B) (143 cGTOs for BF_2), were used for the excitation energy calculations. The diffuse d-functions were added to improve the description of

[†] NIST/NRC Postdoctoral Associate.
[‡] E-mail address: karl.irikura@nist.gov.
[§] E-mail address: jeffrey.hudgens@nist.gov.
[⊗] Abstract published in *Advance ACS Abstracts,* February 15, 1997.

S1089-5639(96)02325-0 This article not subject to U.S. Copyright. Published 1997 by the American Chemical Society

TABLE 1: Relative Energies, Structures, and Vibrational Frequencies Predicted from Frozen-Core QCISD(T)/6-311+G* Calculations (Unmarked) and from B3LYP/6-311+G* Calculations (in Brackets) for BF_2 Radicals, Cations, and Anions

species	energy relationships, eV	r(BF), Å	∠F−B−F, deg	ν_1, cm^{-1}	ν_2, cm^{-1}	ν_3, cm^{-1}
$^{10}BF_2$ ($\tilde{X}\ ^2A_1$)	$IP_a = 8.66$			1152	524	1433
	$IP_v = 10.44$			[1149]	[517]	[1416]
	[$IP_a = 8.32$]	1.317	121.3	(1181.6)[a]	(529.5)[a]	(1442.4)[a]
$^{11}BF_2$ ($\tilde{X}\ ^2A_1$)	[$IP_v = 10.08$]	[1.315]	[121.1]	1123	519	1384
				[1120]	[511]	[1367]
				(1151.4)[a]	(523.7)[a]	(1394)[a]
$^{10}BF_2^+$ ($\tilde{X}\ ^1\Sigma_g^+$)		1.231	180	1017	511	2133
		[1.229]	[180]	[1021]	[495]	[2132]
$^{11}BF_2^+$ ($\tilde{X}\ ^1\Sigma_g^+$)				1017	493	2055
				[1021]	[477]	[2054]
						(2026.1)[a]
$^{10}BF_2^-$ ($\tilde{X}\ ^1A_1$)	$EA = 1.14$			942	519	953
	$VDE = 1.64$	1.401	105.6	[949]	[519]	[935]
$^{11}BF_2^-$ ($\tilde{X}\ ^1A_1$)	[$EA = 1.00$]	[1.397]	[105.3]	914	515	922
	[$VDE = 1.48$]			[920]	[515]	[905]

[a] Experimental value from ref 9.

the 3d Rydberg states and to bring the exponent for the most diffuse d-function into line with those for the most diffuse s- and p-functions. The extra set of diffuse d-functions lowered the CIS excitation energies for the Rydberg d-states of BF by about 1.25 eV and improved the agreement with experiment. For consistency with the diffuse functions of lower *l*, these d-functions were added to boron, instead of the center of charge in the ion.[30] Calculations were performed using the ACES II,[31,32] GAUSSIAN 92/DFT,[33] GAUSSIAN 94,[34] and MOLCAS[35] program packages. Open-shell calculations were spin-unrestricted. All calculations were nonrelativistic and ignored spin−orbit coupling.

Table 1 lists the *ab initio* predictions of the geometries and harmonic vibrational frequencies of the BF_2 radical, cation, and anion calculated at the B3LYP/6-311+G* and frozen-core QCISD(T)/6-311+G* levels. Unmarked values are from the QCISD(T) calculations, values in brackets are from B3LYP calculations, and values in parentheses are the experimental fundamental vibrational frequencies of BF_2 and BF_2^+.[9] The agreement between the sets of *ab initio* and observed frequencies is very good. Experimental frequencies for the anion are unavailable.

Table 1 also contains estimates of the ionization and electron detachment energies for the radical and anion. To compensate for spin and correlation errors, these estimates were calculated using isogyric reaction schemes. At the frozen-core QCISD-(T) level using the 6-311+G(3df)//6-311+G* basis sets, we compute the adiabatic ionization potential of BF_2 to be $IP_a(BF_2)$ = 8.66 eV from the isogyric reaction

$$B^+ + BF_2 \rightarrow B + BF_2^+$$

At the same level and using the isogyric reaction

$$B^- + BF_2 \rightarrow B + BF_2^-$$

we compute the adiabatic electron detachment energy of BF_2^- to be $EA(BF_2)$ = 1.14 eV. At the equilibrium structure of neutral BF_2, similar calculations predict the vertical ionization energy $IP_v(BF_2)$ = 10.44 eV. At the equilibrium structure of BF_2^- the computed vertical electron detachment energy is $VDE(BF_2^-)$ = 1.64 eV. Corresponding values obtained using the B3LYP functional are included in Table 1 between brackets. Adiabatic energy differences include the corresponding vibrational zero-point energies but vertical differences do not. We estimate the ionization energies and detachment energies to be reliable to about 0.05 and 0.1 eV, respectively.

TABLE 2: *Ab Initio* Vertical Excitation Energies (in cm^{-1}) for BF_2[a]

state	CIS	EOM-CCSD	CASPT2(13,13)	B3LYP
$\tilde{X}\ ^2A_1$	0	0	0	0
$1\ ^2B_1[^2\Pi_u]$ (valence)	37 600	35 100	34 700	31 600
$2\ ^2A_1\ [^2\Sigma_g^+]$(3s)	64 800	59 100		
$1\ ^2B_2\ [^2\Sigma_u^+]$ (3p)	69 200	63 100		
$3\ ^2A_1[^2\Pi_u]$ (3p)	69 900	63 100		
$2\ ^2B_1[^2\Pi_u]$ (3p)	72 300	66 000		
$2\ ^2B_2$ (valence)	81 000	71 900	70 100	66 400
$4\ ^2A_1$ (3d)	79 900	72 600		
$3\ ^2B_1$ (3d)	79 800	72 900		
$1\ ^2A_2$ (3d)	80 000	73 300		
$3\ ^2B_2$ (3d)	87 400	73 600		
$5\ ^2A_1$ (3d)	80 700	73 600		
$2\ ^2A_2$ (valence)	94 800	74 800	73 100	69 100

[a] Computations used the aug-cc-pVTZ+d(B) basis set at the B3LYP/6-311+G* geometry of the ground state.

Geometry changes greatly complicate analyses of BF_2 electronic spectra. The ground state geometry of boron difluoride is bent, ∠F−B−F = 121.3°, but the majority of the excited electronic states are linear. The geometry difference between the ground and excited states ($IP_v - IP_a$ = 14 400 cm^{-1}) should cause electronic spectra to display progressions from the ν_2' bending vibration of the upper state. Changes in the BF bond length and BF_2 potential energy surface may also produce a modest progression along the ν_1' symmetric stretch vibration and several combination band progressions of $n*\nu_1' + m*\nu_2'$ (n, m = 0, 1, 2, ...) of the upper state.

Absorption (or emission) spectra are governed by their Franck−Condon envelopes. For BF_2 spectra these envelopes reveal only those vibrational levels far above the origin band and do not allow determination of the spectroscopic constant T_0. To identify the nature of upper electronic states, we must rely upon T_{vert}, the optical transition energy at which the Franck−Condon overlap is at its maximum.[36] T_{vert} is obtained by calculating the excited state energy at the geometry of the ground state radical. Table 2 lists the electronic states of BF_2 and their corresponding values of T_{vert}. The predicted spectroscopic values were obtained at the frozen-core CIS and EE-EOM-CCSD levels. For valence states, T_{vert} values obtained at the CASPT2(13,13) and B3LYP levels are also included in Table 2. The agreement between the CASPT2 and EOM-CCSD results (but not CIS) indicates that the coupled-cluster procedure

TABLE 3: Experimental and *ab Initio* Vertical Excitation Energies for BF[a]

	T_{vert} (cm^{-1})			T_{vert}[calc − expt] (cm^{-1})	
state	expt	CIS	EOM-CCSD	CIS	EOM-CCSD
$\tilde{X}\ ^1\Sigma^+$	0	0	0		
A $^1\Pi$ (valence)	51 440	53 200	52 300	1700	810
B $^1\Sigma^+$ (3s)	66 250	68 700	67 600	2400	1400
C $^1\Sigma^+$ (3p)	69 510	69 900	70 700	300	1100
D $^1\Pi$ (3p)	72 690	73 000	73 600	300	970
E $^1\Delta$ (3d)	76 730	76 700	77 800	−80	970
F $^1\Pi$ (3d)	78 470	77 700	79 000	−800	480
H $^1\Sigma^+$ (3d)	79 340	78 200	79 000	−1200	−400
G $^1\Sigma^+$ (4s)	77 320	91 000	90 600	13 600	13 200

[a] Computations are at the CIS and EE-EOM-CCSD levels using the aug-cc-pVTZ+d(B) basis set. The experimental geometry of the ground state was used.

is successfully accommodating any multideterminant character. Results from the inexpensive B3LYP method ($\langle S^2\rangle \leq 0.76$) are about 3000−6000 cm^{-1} lower than those from the more reliable EOM-CCSD and CASPT2 methods. We note that earlier calculations are in agreement with our results. The vertical excitation energy $^2B_1 \leftarrow \tilde{X}$ has been calculated to be 36 900 cm^{-1} at the MRSDCI/DZP level[18] and 32 000 cm^{-1} at the MRD-CI/TZP+bond+diffuse(B) level.[15,16] The latter calculations also placed the vertical excitation energy $2\ ^2A_1 \leftarrow \tilde{X}\ ^2A_1$ at 57 000 cm^{-1}.[15,16]

To help estimate the accuracy of the excitation energies of BF_2, we calculated a set of T_{vert} for the BF radical at the CIS and EE-EOM-CCSD levels for comparison with experiment. The electronic structures of BF and BF_2 are not similar; this was intended as a test of the quality of the basis set, especially for Rydberg states. "Experimental harmonic T_{vert}" values were computed by assuming harmonic potential curves and using experimental spectroscopic constants, ω_e and r_e.[37] Table 3 lists these results. The experimental geometry $r_e(BF) = 1.2625$ Å was used in the calculations.[37] The basis set appears to describe the valence and $n = 3$ Rydberg states quite well but is inadequate for $n > 3$. Excluding the G state ($n = 4$), the root mean square differences between the computed and experimental vertical excitation energies for BF are 1300 and 890 cm^{-1} for the CIS and EE-EOM-CCSD calculations, respectively. Barring unusual electronic structures, we expect the excitation energies computed for BF_2 to be of comparable accuracy.

Experimental Apparatus and Methods

The experimental apparatus consists of a sampled flow reactor, a pulsed tunable dye laser, a time of flight (TOF) mass spectrometer, and a computer control−data acquisition system.[38] The radicals are produced by reacting atomic fluorine, produced in a microwave discharge (2450 MHz, 30 W) of 5% F_2 in helium, with 10% B_2H_6/90% He, in a large excess of helium. For these studies, the optimized reaction mixture for BF_2 production was found to be 3 Pa (20 mTorr) of B_2H_6, 70 Pa (500 mTorr) of 5% F_2/He, and balance He to produce 200 Pa (1.5 Torr) total pressure. This mixture was allowed to react and was then effusively sampled by a large orifice (∼1 mm) skimmer, while the majority of the gas mixture was pumped away. The effusive flow entered the ion extraction region of the time of flight mass spectrometer where it interacted with the focused pulsed laser beam. The ions were accelerated, focused, mass separated, and detected by a Daly ion detector.[39] Two separate gated integrator/boxcar averagers were used to monitor simultaneously the signals from the two major isotopic products $^{10}BF_2^+$ and $^{11}BF_2^+$. The data were collected and archived by a personal computer. The TOF mass spectrum was displayed on the oscilloscope to ascertain the product masses and to ensure that unit mass resolution was achieved. Differential pumping maintained the base pressure in the ionization region at less than 3 mPa (2×10^{-5} Torr).

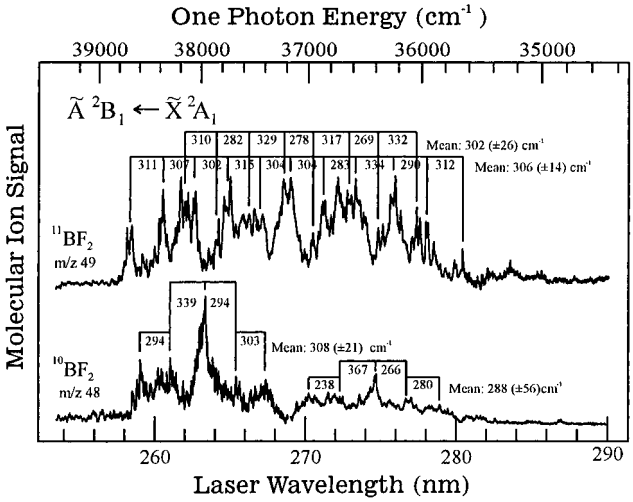

Figure 1. REMPI spectra of $^{11}BF_2$ (*m*/*z* 49) and $^{10}BF_2$ (*m*/*z* 48) between 254 and 290 nm.

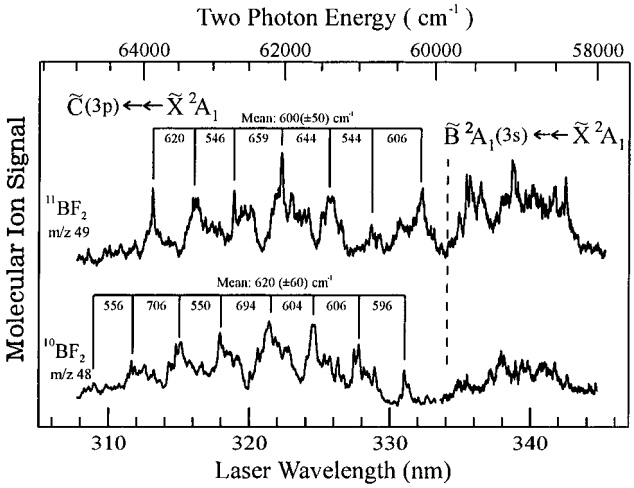

Figure 2. REMPI spectra of $^{11}BF_2$ (*m*/*z* 49) and $^{10}BF_2$ (*m*/*z* 48) between 308 and 344 nm.

To cover the extensive wavelength range presented here, we used a variety of laser dyes, pumped either by a Nd:YAG (10 ns pulse width) or by an XeCl excimer (20 ns pulse width) laser. At wavelengths above 330 nm, the fundamental of the dye laser was used directly. Below this wavelength, the fundamental was frequency-doubled and chromatically separated before use. During these experiments we maintained a nearly constant focal length of 250 ± 5 mm by exchanging lenses as necessary to accommodate the variation of refractive index with wavelength. As is customary, the spectra presented here do not incorporate corrections for laser power variation across the laser dye efficiency profiles; however, the data that comprise these figures were selected to minimize any abrupt signal intensity changes due to laser performance.

Results and Analyses of the Experimental Spectra

a. Proof of the Spectral Carrier. Figure 1 shows the *m*/*z* 48 and *m*/*z* 49 REMPI spectra of BF_2 between 254 and 290 nm and Figure 2 shows the REMPI spectra between 308 and 344 nm. The figures show only the spectral regions that exhibited spectroscopic structure. Broad, featureless *m*/*z* 48 and *m*/*z* 49 ion signals were also observed continuously between 420 and

235 nm and between 440 and 560 nm. In accordance with the ^{11}B:$^{10}B \sim 5$:1 isotopic abundance ratio,[40] the *m*/*z* 49 ion current was approximately 5 times more intense than the *m*/*z* 48 REMPI ion current. The BF_2^+ signals were proportional to the concentrations of fluorine and diborane within the reactor. Whenever the microwave discharge that generated fluorine atoms was extinguished, the BF_2^+ signals ceased. When BF_3 was flowed into the apparatus without a discharge, no ion signal appeared between 255 and 365 nm at any mass. In a second series of experiments, helium and BF_3 mixtures passed through a microwave discharge in a reactor designed to sample the plasma effluent directly into the apparatus. The plasma effluent produced the same *m*/*z* 48 and *m*/*z* 49 REMPI spectra as presented in Figures 1 and 2 and allows us to dismiss spectral contributions from hydrogen-containing species, e.g., BHF_2. Therefore, all chemical evidence supports the assignment of these spectra to the BF_2 radical. Because masses lower than *m*/*z* 48 and *m*/*z* 49 did not carry the spectra of BF_2, we conclude that BF_2^+ does not photodissociate nor does BF_2 dissociatively photoionize when exposed to light between 235 and 560 nm.

The flow reactor effluent exhibited REMPI signals from other boron-containing radicals. Between 304 and 306 nm, BF radicals produced *m*/*z* 29 and *m*/*z* 30 REMPI spectra of the B $^1\Sigma^+(3s) \leftarrow\leftarrow X\ ^1\Sigma^+$ band system.[41,17] Between 310 and 330 nm, the BH radical (*m*/*z* 11 and *m*/*z* 12) exhibited a rotationally-resolved, 2+1 REMPI spectrum of the E $^1\Sigma^+(3p) \leftarrow\leftarrow X\ ^1\Sigma^+$ transition.[37] Between 318 and 337 nm, B_2 radicals produced bands carried by *m*/*z* 20, *m*/*z* 21, and *m*/*z* 22.[17] Between 305 and 330 nm boron atoms produced *m*/*z* 10 and *m*/*z* 11 REMPI spectra involving the np $^2P^o_{1/2,3/2}$ ($n = 5-9$) Rydberg states.[42,17] The REMPI spectra from B atoms and B_2 also demonstrated that free boron is present within the reactor.

b. Analyses of the REMPI Spectra of BF_2 Radicals. Figures 1 and 2 show three distinct band systems originating from $BF_2(\tilde{X}\ ^2A_1)$ radicals to upper states labeled $\tilde{A}$, $\tilde{B}$, and $\tilde{C}$. As expected for species that are changing from bent to linear structures, each band system shows no discernible origin. Each band system displays progressions that arise from the excited state ν_2' bending mode, and each progression shows an apparently staggered vibrational frequency interval. Staggered intervals are consistent with linear−bent transitions to Λ-doubled vibrational levels in triatomic species.[16,43,44]

The $\tilde{A} \leftarrow \tilde{X}\ ^2A_1$ band system (Figure 1) appears between 258 and 282 nm as a set of irregular progressions. EOM-CCSD *ab initio* calculations predict $T_{vert} = 35\,100\ cm^{-1}$ for the 1^2B_1 [$^2\Pi_u$] valence state. This T_{vert} corresponds to one-photon resonances near $\lambda_{laser} = 285$ nm, which coincides with the stronger REMPI bands. Therefore, we assign the upper state as $\tilde{A}\ ^2B_1$. After absorbing a second laser photon, $BF_2(\tilde{X}\ ^2B_1)$ radicals may ionize to form $BF_2^+(\tilde{X}\ ^1\Sigma_g^+)$ cations; i.e., ion signals originate from a 1+1 REMPI mechanism.

The $\tilde{A}^2B_1 \leftarrow \tilde{X}\ ^2A_1$ REMPI bands form poorly-defined progressions. The most suggestive interval is 310 (±20) cm^{-1}, particularly in the $^{10}BF_2$ spectrum. We attribute these progressions to activity in the ν_2' vibrational mode of the $\tilde{A}\ ^2B_1$ state. For the $\tilde{A}\ ^2B_1$ state MRD-CI calculations[16] predict a $\nu_2 = 0-1$ bending frequency of $\nu_2 = 265\ cm^{-1}$ and that the bending mode has negative anharmonicity. The MRD-CI calculations also predict that the most probable transition in the $\tilde{A}\ ^2B_1 \leftarrow \tilde{X}\ ^2A_1$ absorption spectrum is to the $\nu_2' = 19$ level in the $\tilde{A}\ ^2B_1$ state. Thus, when we posit that the REMPI system consists of transitions to vibrational levels near $\nu_2' \sim 19$, the band intervals $\nu_2' = 310$ (±20) cm^{-1} indicate that the spectroscopic constant for negative anharmonicity is about $-1.2\ cm^{-1}$.

The adiabatic ionization potential of BF_2 requires the $\tilde{B} \leftarrow \tilde{X}\ ^2A_1$ and $\tilde{C} \leftarrow \tilde{X}\ ^2A_1$ band systems to arise through absorption of at least three laser photons. The $\tilde{B} \leftarrow \tilde{X}\ ^2A_1$ band system appearing between 334 nm and 350 nm overlaps $\lambda_{laser} = 338$ nm, the two-photon wavelength predicted by our EOM-CCSD calculations for the $2\ ^2A_1$ (3s) $\leftarrow\leftarrow \tilde{X}\ ^2A_1$ vertical excitation ($T_{vert} \sim 59\,100\ cm^{-1}$). The $2\ ^2A_1$ state is predicted to possess primarily 3s Rydberg character.

The $\tilde{B}\ ^2A_1$ (3s) $\leftarrow\leftarrow \tilde{X}\ ^2A_1$ band system shows no regular vibrational progression. MRD-CI calculations[16] predict that vertical excitation into the $2\ ^2A_1$ state is most likely to prepare $\nu_2' = 37$. MRD-CI calculations also predict that the $2\ ^2A_1$ ν_2 manifold is strongly perturbed by avoided crossings. The average vibrational interval rapidly decreases from $\nu_2' = 665\ cm^{-1}$ for $\nu_2' = 1-0$ to $\nu_2' = 553\ cm^{-1}$ for $\nu_2' = 7-6$.[16] Presumably, these perturbations extend to higher levels of the vibrational manifold.

The interplay of alternating REMPI mechanisms as a function of laser wavelength may also contribute to the irregular structure of the $\tilde{B}\ ^2A_1$ (3s) $\leftarrow\leftarrow \tilde{X}\ ^2A_1$ band system. The $\tilde{B}\ ^2A_1$ (3s) $\leftarrow\leftarrow \tilde{X}\ ^2A_1$ band system may appear through a 2+1 REMPI mechanism. In addition, the $\tilde{B}\ ^2A_1$ (3s) $\leftarrow\leftarrow \tilde{X}\ ^2A_1$ band system may obtain resonance enhancement from the $\tilde{A}\ ^2B_1$ state which resides at the one-photon energy. The 1+1+1 REMPI mechanism should dominate at laser wavelengths for which linked $\tilde{A}\ ^2B_1-\tilde{X}\ ^2A_1$ and $\tilde{B}\ ^2A_1$ (3s)$-\tilde{A}\ ^2B_1$ transitions are isoenergetic.

The $\tilde{C} \leftarrow \tilde{X}\ ^2A_1$ band system appears between 310 and 334 nm and overlaps $\lambda_{laser} = 317$ nm, the two-photon wavelength predicted by EOM-CCSD calculations for the $2\ ^2B_2$ and $3\ ^2A_1$ vertical excitations ($T_{vert} \sim 63\,100\ cm^{-1}$ for both states). These states possess primarily 3p Rydberg character. No high-level calculations have predicted the vibrational manifolds of these states. If these states are unperturbed, we expect their vibrations to approximate those of BF_2^+ ($\omega_2 = 511\ cm^{-1}$) and their vertical excitation energies to center on $\nu_2' = (IP_v - IP_a)/\omega_2' \approx 30$. The $^{10}BF_2$ and $^{11}BF_2$ spectra exhibit irregular vibrational progressions with average intervals of $\nu_2' = 603\ cm^{-1}$ and $\nu_2' = 616\ cm^{-1}$, respectively. This vibrational frequency is greater than the cation frequency, a result which may arise either from perturbations or because the ν_2 bending mode has a small negative anharmonicity. MRD-CI calculations predict that the $\tilde{A}\ ^2B_1 \leftarrow \tilde{X}^2A_1$ system can provide resonance enhancement at the one-photon energy. However, the intensity pattern of the $\tilde{C}\ ^2\Pi$ (3p) − $\tilde{X}\ ^2A_1$ band system is fairly simple and does not show the irregular intensity enhancements that 1+1+1 REMPI mechanisms should contribute. Therefore, we conclude that the $\tilde{C}\ ^2\Pi$ (3p) $\leftarrow \tilde{X}\ ^2A_1$ transitions occur solely through the 2+1 REMPI mechanism.

Conclusion

As noted earlier in the Introduction, the use of boron-containing compounds in CVD and by the semiconductor industry has prompted renewed interest in the structure and properties of simple boron-containing radicals. These radicals are additionally attractive to theoretical workers due to their inherent simplicity. Unfortunately, little experimental work has been conducted on these radicals, and therefore the results of high-level CI calculations have remained largely untested. This report constitutes such experimental work. New calculations of the ground state geometries and the vibrational frequencies of the radical, cation, and anion are presented, some of which have been verified by matrix isolation experiments.[9] The vertical transition energies to the excited electronic states at the ground state equilibrium geometry have been calculated for BF and BF_2 and good agreement with experiment is demonstrated

for BF. The results for BF_2 have been very useful in the interpretation of the current REMPI results. The REMPI technique represents an extremely sensitive, selective, and generally applicable detection scheme for BF_2. The applicability of the technique stems in part from the wide range of wavelengths that produce ionization.

Acknowledgment. We thank Dr. Russell D. Johnson III for many helpful discussions regarding interpretation of the spectra and calculations. We also thank Dr. Herb Nelson of the Naval Research Laboratory for advice during the experimental studies.

References and Notes

(1) Yarbrough, W. A. *J. Vac. Sci. Technol.* **1991**, *A9*, 1145−1152.
(2) Nisimura, K.; Das, K.; Glass, J. T. *J. Appl. Phys.* **1991**, *69*, 3142.
(3) Kinoshita, T.; Takakura, M.; Miyazaki, S.; Yokoyama, S.; Koyanagi, M.; Hirose, M. *Jpn. J. Appl. Phys.* **1990**, *29*, L2349.
(4) Lin, C.-Y.; Chang, C.-Y.; Hsu, C. C.-H. *IEEE Trans. Electron Dev.* **1995**, *42*, 1503.
(5) Zhao, Q.-T.; Wang, Z.-L.; Cao, Y.-M.; Xu, T.-B.; Zhu, P.-R. *J. Appl. Phys.* **1995**, *77*, 5014.
(6) Zhao, Q.-T.; Wang, Z.-L.; Xu, T.-B.; Zhu, P.-R.; Zhou, J.-S. *Appl. Phys. Lett.* **1994**, *64*, 175.
(7) Wu, I.-W.; Fulks, R. T.; Mikkelsen Jr., J. C. *J. Appl. Phys.* **1986**, *60*, 2422.
(8) Hassanzadeh, P.; Andrews, L. *J. Phys. Chem.* **1993**, *97*, 4910.
(9) Jacox, M. E.; Thompson, W. E. *J. Chem. Phys.* **1995**, *102*, 4747−4756.
(10) Nelson, W.; Gordy, W. *J. Chem. Phys.* **1969**, *51*, 4710−4713.
(11) Creasey, J. C.; Hatherly, P. A.; Jones, H. M.; Lambert, I. R.; Tuckett, R. P. *Mol. Phys.* **1993**, *78*, 837−854.
(12) Suto, M.; Ye, C.; Lee, L. C. *Phys. Rev. A* **1990**, *42*, 424−431.
(13) Hesser, J. E.; Dressler, K. *J. Chem. Phys.* **1967**, *47*, 3443−3450.
(14) Krishnamachari, S. L. N. G.; Narasimham, N. A.; Singh, M. Proceedings of the International Conference on Spectrometry, 1967, Bombay.
(15) Perić, M.; Peyerimhoff, S. D. *Mol. Phys.* **1993**, *78*, 855−875.
(16) Perić, M.; Peyerimhoff, S. D. *Mol. Phys.* **1993**, *78*, 877−892.
(17) Hudgens, J. W.; Irikura, K. K.; Johnson III, R. D. "New Spectroscopy of Free Radicals Produced by the Reactions of Fluorine and Chlorine with Diborane"; SPIE-Laser Techniques for State-Selected and State-to-State Chemistry II, 1994, Los Angeles, CA.
(18) Cai, Z.-L. *Int. J. Quantum Chem.* **1993**, *45*, 295−301.
(19) Thomson, C.; Brotchie, A. *Theor. Chim. Acta* **1973**, *32*, 101.
(20) Thomson, C.; Brotchie, A. *Chem. Phys. Lett.* **1972**, *16*, 573.
(21) Rothenberg, S.; Schaefer III, H. F. *J. Am. Chem. Soc.* **1973**, *95*, 2095.
(22) Baird, N. C.; Kuhn, M.; Lauriston, T. M. *Can. J. Chem.* **1989**, *67*, 1952.
(23) Pople, J. A.; Head-Gordon, M.; Raghavachari, K. *J. Chem. Phys.* **1987**, *87*, 5968−5975.
(24) Raghavachari, K. *Annu. Rev. Phys. Chem.* **1991**, *42*, 615−642.
(25) Stephens, P. J.; Devlin, F. J.; Chabalowski, C. F.; Frisch, M. J. *J. Phys. Chem.* **1994**, *98*, 11623−11627.
(26) Stanton, J. F.; Bartlett, R. J. *J. Chem. Phys.* **1993**, *98*, 7029−7039.
(27) Andersson, K.; Malmqvist, P.-Å.; Roos, B. O. *J. Chem. Phys.* **1992**, *96*, 1218−1226.
(28) Dunning, T. H., Jr. *J. Chem. Phys.* **1989**, *90*, 1007−1023.
(29) Kendall, R. A.; Dunning, T. H., Jr. *J. Chem. Phys.* **1992**, *96*, 6796−6806.
(30) Roos, B. O.; Andersson, K.; Fülscher, M. P.; Malmqvist, P.-Å.; Serrano-Andrés, L. *Adv. Chem. Phys.* **1996**, *93*, 219−331.
(31) ACES II, an ab initio program system authored by J. F. Stanton, J. Gauss, J. D. Watts, W. J. Lauderdale, and R. J. Bartlett. The package also contains modified versions of the MOLECULE Gaussian integral program of J. Almlöf and P. R. Taylor, the ABACUS integral derivative program of T. U. Helgaker, H. J. A. Jense, P. Jorgensen, and P. R. Taylor, and the PROPS property integral package of P. R. Taylor.
(32) Stanton, J. F.; Gauss, J.; Watts, J. D.; Lauderdale, W. J.; Bartlett, R. J. *Int. J. Quant. Chem.* **1992**, *S26*, 879−894.
(33) *Gaussian 92/DFT*. Frisch, M. J.; Trucks, G. W.; Schlegel, H. B.; Gill, P. M. W.; Johnson, B. G.; Wong, M. W.; Foresman, J. B.; Robb, M. A.; Head-Gordon, M.; Replogle, E. S.; Gomperts, R.; Andres, J. L.; Raghavachari, K.; Binkley, J. S.; Gonzalez, C.; Martin, R. L.; Fox, D. J.; Defrees, D. J.; Baker, J.; Stewart, J. J. P.; Pople, J. A. Gaussian, Inc., Pittsburgh, PA, 1993.
(34) *Gaussian 94*. Frisch, M. J.; Trucks, G. W.; Schlegel, H. B.; Gill, P. M. W.; Johnson, B. G.; Robb, M. A.; Cheeseman, J. R.; Keith, T.; Petersson, G. A.; Montgomery, J. A.; Raghavachari, K.; Al-Laham, M. A.; Zakrzewski, V. G.; Ortiz, J. V.; Foresman, J. B.; Cioslowski, J.; Stefanov, B. B.; Nanayakkara, A.; Challacombe, M.; Peng, C. Y.; Ayala, P. Y.; Chen, W.; Wong, M. W.; Andres, J. L.; Replogle, E. S.; Gomperts, R.; Martin, R. L.; Fox, D. J.; Binkley, J. S.; Defrees, D. J.; Baker, J.; Stewart, J. P.; Head-Gordon, M.; Gonzalez, C.; Pople, J. A. Gaussian, Inc., Pittsburgh, PA, 1995.
(35) *MOLCAS version 3*. Andersson, K.; Blomberg, M. R. A.; Fülscher, M. P.; Kellö, V.; Lindh, R.; Malmqvist, P.-Å.; Noga, J.; Olsen, J.; Roos, B. O.; Sadlej, A. J.; Siegbahn, P. E. M.; Urban, M.; Widmark, P.-O. University of Lund, Sweden, 1994.
(36) Because rapid dissociation and nonradiative relaxation from the intermediate state may quench the production of ion signal, T_{vert} is not required to coincide with the energy of maximum REMPI signal. However, in this paper no effects from these nonradiative process are obvious and T_{vert} is treated as the energy of maximum signal.
(37) Huber, K. P.; Herzberg, G. *Molecular Spectra and Molecular Structure: IV. Constants of Diatomic Molecules*; van Nostrand Reinhold: New York, 1979.
(38) Johnson, R. D., III; Tsai, B. P.; Hudgens, J. W. *J. Chem. Phys.* **1988**, *89*, 4558.
(39) Daly, N. R. *Rev. Sci. Instrum.* **1960**, *31*, 264.
(40) Heath, R. L. Table of the Isotopes. In *CRC Handbook of Chemistry and Physics*, 64th ed.; Weast, R. C., Astle, M. J., H., B. W., Eds.; CRC Press, Inc.: Boca Raton, FL, 1984; Vol. 64.
(41) Irikura, K. K.; Johnson, R. D., III; Hudgens, J. W. *Appl. Phys. Lett.* **1993**, *6*, 1697.
(42) Irikura, K. K.; Johnson, R. D., III; Hudgens, J. W. *J. Opt. Soc. B* **1993**, *10*, 763.
(43) Ritchie, R. K.; Walsh, A. D. *Proc. R. Soc.* **1962**, *267 A*, 395−407.
(44) Herzberg, G. *Molecular Spectra and Molecular Structure III. Electronic Spectra and Electronic Structure of Polyatomic Molecules*; Van Nostrand Reinhold Co.: New York, 1966.